

The Varying Core Magnetic Field from a Space Weather Perspective

Mioara Manda¹ · Michael Purucker²

Received: 2 April 2017 / Accepted: 13 November 2017 / Published online: 30 November 2017
© Springer Science+Business Media B.V., part of Springer Nature 2017

Abstract This paper summarizes recent advances in our understanding of geomagnetism, and its relevance to terrestrial space weather. It also discusses specific core magnetic field features such as the dipole moment decay, the evolution of the South Atlantic anomaly, and the location of the magnetic poles that are of importance for the practice of space weather.

Keywords Core field · Secular variation · Secular acceleration · Dipole decay · South Atlantic Anomaly

1 Introduction

The geometry of the geomagnetic field, and its evolution in space and time contribute to the complexities of space weather observed at the surface of the Earth, and in the near-Earth space. This paper is devoted to a review of our knowledge of the geomagnetic field as it pertains to a better understanding of space weather effects. Space weather is defined as the collection of physical processes, beginning at the Sun, and ultimately affecting human activities on Earth and in space (Natural Resources Canada 2017). Radiation and particles emitted from the Sun, with variable delays, interact with the geomagnetic field, and the atmosphere, in ways that cause electrical currents to flow in regions of the ionosphere and magnetosphere. The radiation and particles also contribute to energetic particle populations in the near-Earth space. The electrical currents, and the changing energetic particle populations result in geomagnetic variations, aurora, and can profoundly affect a number of technologies.

The Scientific Foundation of Space Weather
Edited by Rudolf von Steiger, Daniel Baker, André Balogh, Tamás Gombosi, Hannu Koskinen and Astrid Veronig

✉ M. Manda
mioara.manda@cnes.fr

¹ CNES—Centre National d'Etudes Spatiales, 2 Place Maurice Quentin, 75039 Paris, France

² NASA—Goddard Space Flight Center, Greenbelt, MD 20771, USA

The geomagnetic field can be described in terms of magnetic poles. These poles are either deduced from the dipole term exclusively, and dominate within the plasma source regions in the magnetic tail that feed the auroral oval, or they include higher-order terms, and can describe the near-Earth fields. The northern and southern magnetic poles change positions with time, and these changes affect the location of the auroral ovals, the cusp, the location of open and closed field lines, and where those field lines connect. On a global scale, the decay of the geomagnetic field over the past few centuries has engendered a significant change in the near-Earth radiation environment. For example, the expansion of the well-known South Atlantic anomaly (SAA) creates more single-event upsets (SEU) in the electronics systems of near-Earth satellites.

To understand the Earth's complicated magnetic environment, a tour is needed through the origins of the geomagnetic field. The Earth's magnetic field comprises contributions from sources inside the Earth (internal contributions) and outside it (external contributions). Internal sources include the core field (also called the main field) originating in the external fluid core of the Earth) and the lithospheric field (caused by magnetic minerals in the crust and subordinately the upper mantle). The external sources have their origins in the ionosphere, the magnetosphere and also from electrical currents coupling the ionosphere and magnetosphere (field aligned currents, or FAC). These sources external to the solid Earth induce secondary fields in the Earth. The core magnetic field acts like a shield to the solar wind that the Sun continually emits. The need to understand the variations of the core field is then essential when space weather is considered. However, to analyze the core field and its variations, we also need to understand the interactions and separations of different geomagnetic field sources. The data and tools to obtain the best possible description of the magnetic field constituents are multi-faceted, so their review can bring us the capability to better describe and understand core field variations.

To take into consideration these issues, the remainder of the paper is organized as follows. Section 2 looks at the Earth's magnetic field contributions and how to measure them on the ground and in the near-Earth space. In Sect. 3 some information on modeling the magnetic field is given, mainly to show the possibilities to describe the core field. Section 4 discusses the core field and its variations, and finally Sect. 5 draws some conclusions and maps out future directions.

2 The Magnetic Field: Sources and Measurements

2.1 Geomagnetic Field Sources

The sources of internal magnetic fields include those originating in the core and lithosphere of the Earth. These natural magnetic fields largely originate in electric currents and magnetized media, respectively. The core field (Hulot et al. 2015) is dominated by a field generated from a self-sustaining dynamo in the Earth's molten outer core. The lithospheric fields (Purucker and Whaler 2015) are generated in rocks from the upper portion of the Earth's lithosphere that remain below the Curie temperature and containing minerals carrying the magnetization. The largest scale, and magnitude of these formally inseparable core and lithospheric fields can be approximated by an offset magnetic dipole at some distance from the Earth's rotation axis. The strongest scalar magnetic fields originating from the Earth's core are found in the Earth's polar regions. The area just offshore Antarctica, in the ocean between Australia and the Antarctic, possesses the largest scalar magnetic fields, averaging 66000 nT.

In contrast, the magnetic fields originating from the Earth's lithosphere have a bimodal character, lineated above the ocean lithosphere and weaker than the fields associated with continental lithospheres, which are characterized by much more varied patterns. At the surface of the Earth, the weak oceanic lithospheric fields are dominantly a function of the difference in thickness of the oceanic vs. continental crust (7 vs. 35 km, respectively). Two kinds of magnetization can exist within the cool lithosphere, permanent (remanent) magnetization and induced magnetization. The direction and intensity of permanent magnetization is dependent on the origin and history of the rock. Induced magnetization is proportional in magnitude, and generally parallel to the ambient core field. Another first-order observation about the strength of the lithospheric field is that the field, while variable in detail, varies in magnitude from the magnetic poles to the equator by a factor of two, a reflection of a strong contribution from induced magnetization.

The sources of external magnetic fields include those originating in the ionosphere, those which couple the magnetosphere and ionosphere, and those associated with more distant regions of the magnetosphere, for example the ring current, the magnetotail, and the magnetopause. These fields are produced by electric current systems in the ionosphere and magnetosphere. These current systems in the ionosphere originate in currents driven by dynamo processes in the ionospheric plasma. In the magnetosphere, currents are often produced by the movement of charged particles. The magnitude of these fields at the surface varies in local time (LT), in space, and in response to solar forcing. At ground level, a large-scale magnetospheric field of some tens of nT is found at all times. The ionospheric field at ground level in magnetically quiet times is of the order of a few nT or so, and varies with LT, with a maximum of several tens of nT associated with a commonly known Solar quiet (Sq) variation, a consequence of electric currents flowing in the region of ionosphere between some 90–150 km (Campbell 2003). In disturbed magnetic conditions, ionospheric and magnetospheric fields become much larger, and more dynamic, and can reach magnitudes of hundreds, or even thousands, of nT, at the ground. The Carrington solar event in 1859, the largest recorded solar magnetic event, has been associated with external field changes of more than 1500 nT at the Colaba Indian magnetic observatory (Cliver and Dietrich 2013).

2.2 Measuring the Geomagnetic Field

Measurements of the geomagnetic field include archeomagnetic and paleomagnetic time series for magnetic intensity, marine compass records for magnetic declination, magnetic observatories for vector measurements, and since the 1960s, near-Earth satellites measuring the scalar magnetic field, and only since the end of the 1970s the vector magnetic field. Human observations of the geomagnetic field began with measurements of declination (D) less than 500 years ago. One of the longest time series is Paris one. The declination and its first time derivative (secular variation) for the Paris series (Alexandrescu et al. 1996; Mandaia and Le Mouél 2016) is plotted in Fig. 1. This figure shows that the declination varies over tens of degrees over a couple of centuries. Of course the interest is to be able to characterize these variations at a global scale and to understand them. The declination measurements expanded to measurements of inclination (I) some 400 years ago.

It has been less than 200 years, since 1832, that Gauss demonstrated the ability to measure the absolute intensity of the geomagnetic field, and the first magnetic observatories were installed. Magnetic observatories require a full description of the geomagnetic field so two types of measurements are needed: vector and scalar. The vector measurements are generally made with a fluxgate magnetometer, and they are subject to instrument drift. To minimize this drift a scalar magnetometer is used in a calibration procedure. A type of proton

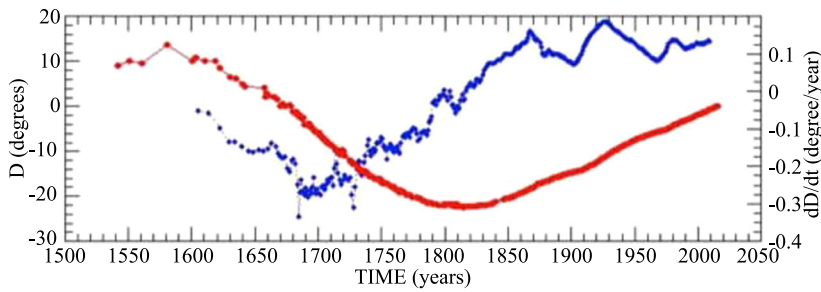


Fig. 1 Paris series: Annual mean values of declination for the period 1541–2015 (D , red curve, left vertical axis), adjusted for the Chambon la Forêt observatory location. The secular variation is computed by annual differences starting with 1600 and applying an 11-yr smoothing (dD/dt , blue curve, right vertical axis)

precession or resonance magnetometer, such as the Overhauser magnetometer, is typically installed at magnetic observatories to measure the field intensity. Such a device, however, makes measurements of the strength of the magnetic field only, and provides no information about its direction. To complete a set of measurements information about the direction of the geomagnetic field is needed, obtained by measuring the declination and inclination, commonly using a fluxgate-theodolite (named Declination Inclination fluxgate, or DI-flux).

Modern magnetic observatories use similar instrumentation to produce similar data products (Intermagnet 2017). For many observatories the fundamental measurements recorded are one-second values, used thereafter to compute one-minute values of the vector components and of scalar intensity. From the one-minute data, hourly, daily, monthly and annual mean values are produced. The magnetic field variation over a day gives an important indication about the status of the day, i.e. a magnetically “disturbed” or “quiet” day. An example is given in Fig. 2, the choice being to show the “Halloween” geomagnetic storm in October 2003, and a quiet day, in October 2016.

Future observatory developments might include remote sensing of the scalar magnetic field (Kane et al. 2016) in the mesosphere at some 90 km altitude based on sodium atoms, the residue of meteor ablation. These laser-based instruments might be included in selected observatories to capture the time variation of the scalar magnetic field close to the ionosphere.

High accuracy and precision measurements of the near-Earth geomagnetic field from space began with NASA’s MAGSAT satellite that flew for six months from 1979 to 1980. This was followed in the first decade of the 21st century by the Ørsted (2017), CHAMP (2017), and SAC-C magnetic field satellites.

Swarm, the 3-satellite ESA constellation (ESA 2017), is the most current, and most advanced geomagnetic observatory in space. One of the novelties of the mission is not only the constellation concept, but also the new absolute scalar magnetometer, an optically pumped Helium magnetometer, which provides absolute scalar measurements of the magnetic field with high accuracy and stability for the calibration of the vector field magnetometer (Leger et al. 2009). The mission was designed to derive the first global representation of the geomagnetic field variations on times scales from an hour to several years, addressing the crucial problem of source separation. The three Swarm satellites are identical, and the constellation consists of two satellites (A and C) flying almost side-by-side at an altitude close to 460 km (April 2016), longitude separation of 1.4 degrees and on circular and almost polar orbits with an inclination of 87.4 degrees. The third satellite (B) flies higher, close to

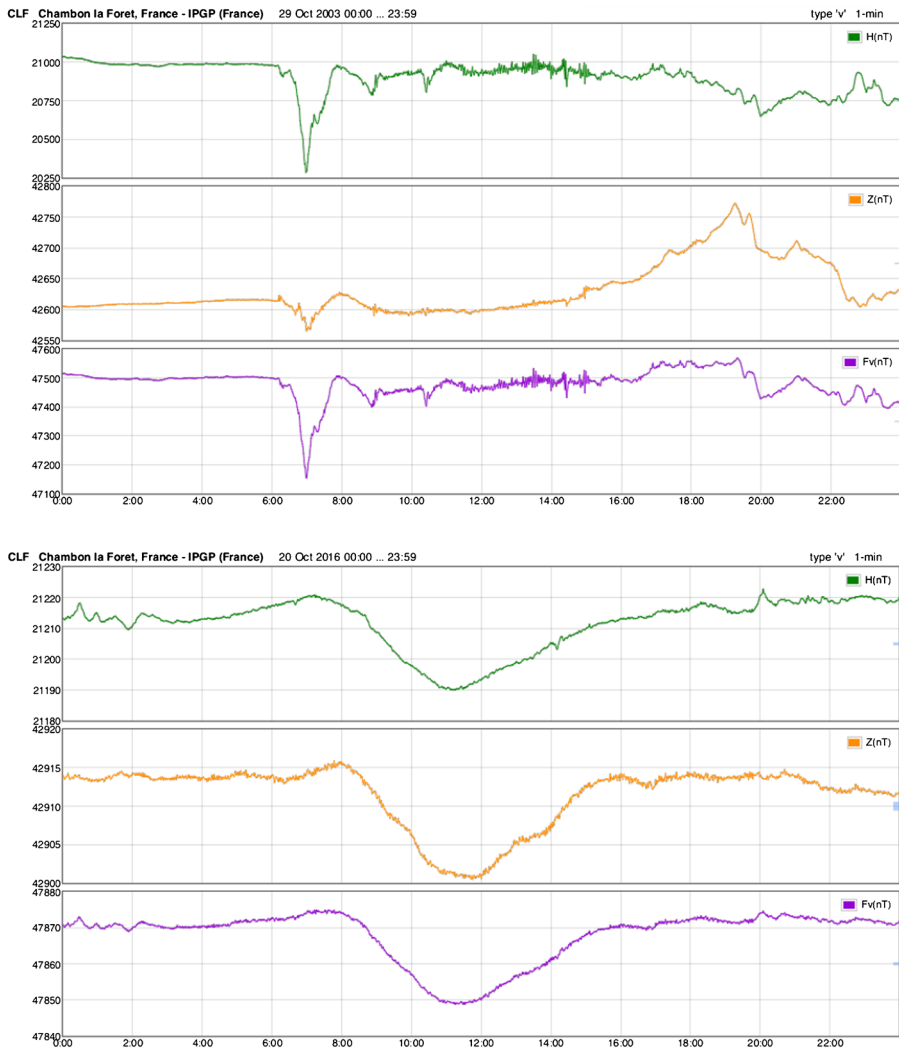


Fig. 2 Magnetograms for a disturbed day (29 October 2003) and a quiet day (20 October 2016), as recorded at Chamon la Forêt observatory (H —horizontal component, Z —vertical component and F —field intensity). Note the differences for the vertical axis

510 km (April 2016), on a more polar orbit (inclination of 87.8 degrees) and is progressively separated in LT with respect to A and C.

As mentioned above, the Swarm magnetometers measure a superposition of magnetic fields produced by a number of different sources: core, lithosphere, ionosphere, and magnetosphere. Note that contributions due to external sources depend largely on latitude, LT, and solar activity, and that other satellites have the capability of making highly precise and accurate magnetic field measurements with fluxgate magnetometers within the magnetosphere or ionosphere. Examples include Cluster (2017), MMS (2017), and the Van Allen Probes (RBSP 2017). These can augment the results of the Swarm mission in the distant magnetosphere, and illuminate the process of magnetic reconnection for example.

The Swarm mission may continue to operate until the 2030s, when the lower two satellites will reenter the atmosphere, leaving only the higher altitude satellite. In order to be assured of high-quality geomagnetic field data in the future, it is important to develop concepts for future missions now. One possibility is the use of one or more CubeSats with scalar Helium magnetometers, a concept under development with support from CNES (Hulot 2017). This implies new instrument developments, including the need to miniaturize the optically pumped Helium magnetometer. Diamond vector magnetometry, using nitrogen-vacancy centers in diamond (Wolf et al. 2015) is another promising class of absolute scalar and vector magnetometers that may see use in observatories and satellite missions of the future.

3 Magnetic Field Modeling

Geomagnetic field modeling in the satellite era has taken many approaches. Those that use large quantities of satellite data directly in inversions or parameter searches often use some combination of selected quiet-time satellite observations and magnetic observatory data, and often use spherical harmonic basis functions, or more localized functions like wavelets. Here, we provide details of the modeling approaches in order to provide the interested reader with an overview of the process. This is useful in space weather practice and we provide regions of validity of the models, and their accuracy and resolution. The time-varying core magnetic field, and models that describe it, are relevant to space weather because they determine where space weather effects are most severe.

Spherical harmonic functions allow us to describe the geomagnetic field as a global phenomenon. The magnetic field, following Maxwell's equations, is source-free, so it can be written:

$$\nabla \times \mathbf{H} = \mathbf{J} + \frac{\partial \mathbf{D}}{\partial t} \quad (1)$$

$$\nabla \cdot \mathbf{B} = 0 \quad (2)$$

where \mathbf{H} is the magnetic field, \mathbf{B} is the magnetic induction, \mathbf{J} is the current density, and $\partial \mathbf{D} / \partial t$ is the electric displacement current density. In a region without magnetic field sources, say from the Earth's surface up to about 50 km, it is reasonable to assume that $\mathbf{J} = 0$ and $\partial \mathbf{D} / \partial t = 0$, so $\nabla \times \mathbf{H} = 0$, meaning that the vector field is conservative in the region of interest, and the magnetic field \mathbf{H} can be expressed as $\mathbf{H} = -\nabla V$, where V is a scalar potential. Because $\mathbf{B} = \mu_0 \mathbf{H}$ above the Earth's surface (where $\mu_0 = 4\pi \times 10^{-7} \text{ Hm}^{-1}$), it follows that $\nabla \cdot \mathbf{H} = 0$ and that V has to satisfy Laplace's equation:

$$\nabla^2 V(\theta, \varphi, r) = 0 \quad (3)$$

In geomagnetism the magnetic induction \mathbf{B} is traditionally called "magnetic field". We use the same notation in the following. In spherical coordinates (θ, φ, r) , which are the geocentric co-latitude, longitude, and radial distance, the solution to Laplace's equation takes the form:

$$\begin{aligned} V &= V^{\text{int}} + V^{\text{ext}} \\ &= a \sum_{n=1}^{N_{\text{int}}} \sum_{m=0}^n (g_n^m \cos m\varphi + h_n^m \sin m\varphi) \left(\frac{a}{r}\right)^{n+1} P_n^m(\cos \theta) \end{aligned}$$

$$+ a \sum_{n=1}^{N_{\text{ext}}} \sum_{m=0}^n (q_n^m \cos m\varphi + s_n^m \sin m\varphi) \left(\frac{r}{a}\right)^n P_n^m(\cos\theta) \tag{4}$$

where $a = 6371.2$ km is a reference radius, (θ, φ, r) , are geocentric coordinates, $P_n^m(\cos\theta)$ are the associated Schmidt-normalized Legendre functions, N_{int} is the maximum degree and order of the internal potential coefficients g_n^m, h_n^m , and N_{ext} is that of the external potential coefficients q_n^m, s_n^m . Note that this equation is expressed in such a form so as to formally separate two important contributions in the potential field: a part, V^{int} describing the internal (core and lithospheric) sources, and a part, V^{ext} describing the external (mainly magneto-spheric) sources.

The Gauss coefficients can be interpreted in terms of “sources”. The first term, g_1^0 , is associated with the geocentric dipole oriented along the vertical axis, i.e. axis of the Earth’s rotation, with dipole moment $g_1^0 4\pi/\mu_0$. The potential for a dipole falls off as r^{-2} and the strength of the field components as r^{-3} . The next two terms, g_1^1, h_1^1 , characterize the geocentric dipole oriented along the two last orthogonal axis. Similarly, for $n = 2$ the terms represent the geocentric quadrupole, for $n = 3$ the terms represent the geocentric octopole, and so forth.

To describe only the part of the geomagnetic field with sources beneath the Earth’s surface, only the part V^{int} of Eq. (4) is used. However, this first term of Eq. (4) describes both the core and lithospheric fields. It is possible to see the transition from magnetic fields originating dominantly in the core from those originating in the lithosphere by computing the mean square value of the field over the Earth’s surface produced by harmonics of a given degree n (Lowes 1966):

$$W_n = (n + 1) \sum_m ((g_n^m)^2 + (h_n^m)^2) \tag{5}$$

Variation of the power W_n depends on degree n and is known as the power or Lowes-Mauersberger spectrum. The steep part of the spectrum ($n \leq 13$) indicates the signature of the long wavelengths of the core field, and the much weaker signatures of the long wavelengths of the lithospheric field. The transition degrees ($n = 14-15$) can be attributed to sub-equal signals from both the core and lithospheric sources, and the higher degrees ($n \geq 16$) are dominantly lithospheric in origin. Examples of models based on spherical harmonics include the IGRF series, the CHAOS series (Olsen et al. 2014; Finlay et al. 2016a, 2016b), the Comprehensive models (Sabaka et al. 2015), and the GRIMM series (Lesur et al. 2015). The attributes of these models are described in Table 1 (Appendix). The newest release of CHAOS and GRIMM models are built along the same lines as their previous versions.

The most widely used magnetic field models are those of the IGRF series (International Geomagnetic Reference Field). Released every five years, they describe the Earth’s core field and its secular variation. The core field is described to spherical harmonic degree 13, and the secular variation is described up to spherical harmonic degree 8 (Table 1). The purpose of the IGRF, and their relative, the World Magnetic Model (WMM) is as a practical way to predict the core field. The uses are myriad but they are focused on navigation, and as a supplement to GPS. The IGRF models are derived from candidate models submitted by independent worldwide teams. The candidates are assessed, and the final model is generally a weighted mean of the candidate models. The virtue of the IGRF is its simplicity, and the candidate models are often simplified and truncated models of more advanced models (cf. Gillet et al. 2015a, 2015b) used to describe the geomagnetic field. We discuss those next.

The more advanced models (Olsen et al. 2014; Finlay et al. 2016a, 2016b; Sabaka et al. 2015; Lesur et al. 2015) use the process of coestimation, and robust least-squares estimation,

to separate the sources of the field. They differ in whether they describe quiet and disturbed magnetic conditions (the Comprehensive model series), or only quiet magnetic conditions (CHAOS and GRIMM). The Comprehensive model is the only model to use data from all local times, and all latitudes. All three of these models use vector and scalar magnetic observations from the CHAMP, Ørsted and SAC-C satellites over the first decade of the 21st century, and hourly or monthly mean observations from the 150 or so magnetic observatories. However, the latest variant of the GRIMM model (Lesur et al. 2015) does not use observatory data. Instead, it uses the observatory data to provide an independent set of measurements with which to test their models. Indeed, the secular variation values estimated from the observatories show a good fit to the model predictions. We illustrate many of our points in subsequent section using the latest model published by Lesur et al. (2015). This model has been specifically designed with the goal of improving the time-varying part of the core magnetic field.

Spherical harmonic analyses are widely used in representing the magnetic field and its variations at the Earth's surface. Here, because of the interest in the manner the radial magnetic field can be represented at the core-mantle boundary (see Sect. 4), these quantities are plotted in Fig. 3.

Another prominent category of models are those which use data assimilation techniques adapted from weather forecasting in an attempt to forecast the state of the core magnetic field years into the future, or into the past using historical databases (Fournier et al. 2010). These inverse methods rely on a numerical model of core dynamics that can be used to predict secular variation at the Earth's surface from the initial conditions. The goal of geomagnetic data assimilation is to combine the geomagnetic data sets with a dynamic numerical model by adjusting the trajectory of the model to adequately fit the data. Many of these models take as their starting point not the measurements of the fields themselves, but rather the models described in the previous paragraphs. The term "data assimilation" in meteorology describes the inverse techniques used to improve the forecast of atmospheric flow, and the state of the atmosphere. In geomagnetism, the observations directly access a much smaller fraction of the state vector than they do in meteorology. To illustrate this statement, the only "observations" that geomagnetism can bring to bear on the state of the core magnetic field are an estimate of the radial magnetic field, and its time derivative, at the core-mantle boundary. Those observations are generated by downward continuing magnetic observations from the surface, using regularization. We also lack knowledge of the background state of the core, the equivalent of a "climatological mean", about which the dynamics is likely to take place. In spite of these limitations, several promising approaches are evident. In particular, the assimilation of laboratory observations of liquid metal analogs of the Earth's core (Adams et al. 2015) offer the promise of both characterizing an appropriate background state, and perhaps offering access to more of the state vector of the core. The approach of Whaler and Beggan (2015) is another promising, and less computationally demanding, approach for short period (< 5 years) prediction, and generates core surface flow models that can be used for forecasting secular variation. The work of Aubert (2015) is the longest-term geomagnetic forecast using data assimilation, extending out a century. This model predicts that the focal (or minimum intensity) point of the South Atlantic Anomaly, discussed later in Sect. 4.3, is predicted to enter the South Pacific region in the next century, with the feature deepening and widening.

Models based on data from the pre-satellite era include the *gufm* model series (Jackson et al. 2000) and the *CALSK-x* model series (Korte et al. 2011). Using historic data from the last 400 years, largely land observatory records and ship navigation data, the *gufm* model is a spherical harmonic model extending to degree 14. The *gufm-sat* model (Finlay et al. 2012)

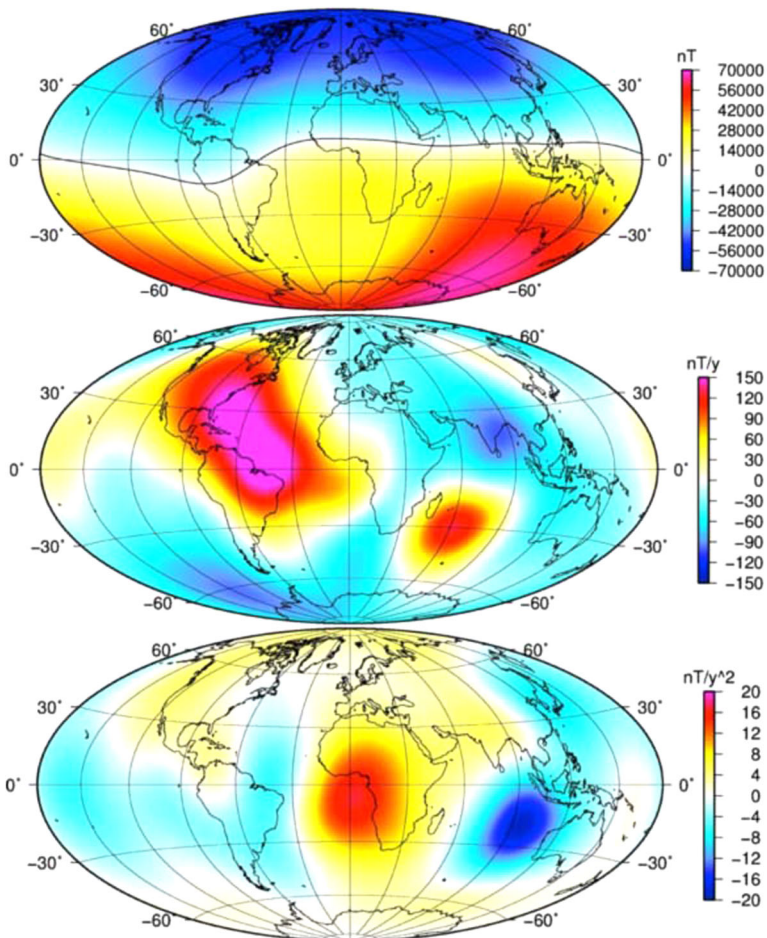


Fig. 3 Radial component of the magnetic field and its variations (secular variation and secular acceleration) at the Earth's surface as obtained from the model by Lesur et al. (2015)

is a potential successor to *gufm*, and incorporates satellite data from the modern era, with a similar parameterization to that of *gufm*. The *CALSK-x* model series is also a spherical harmonic model but uses paleo- and archeomagnetic data, and covers the last few thousand years, with some recent models extending back to a hundred thousand years. The model extends to degrees 8 to 10, but it is based on a very geographically restricted set of data that covers mainly the northern hemisphere.

4 The Core Field and Its Variations

After summarizing the geomagnetic field sources and modeling techniques, we turn to a discussion of core field variations and some of its specific features.

The geomagnetic field is in a permanent state of change on time scales ranging from milliseconds to millions of years. The shortest time scales are linked to processes arising

in the ionosphere and magnetosphere, and their coupling. The longer changes, over time-scales of months to decades, mostly reflect changes in the Earth's core, and the very long ones, from centuries to millions of years, reveal different aspects of core processes.

A dramatic change in the core field is the reversal of its polarity, or, sometimes, an important decrease of its intensity without reaching the reversed, antiparallel, directional state—so-called excursions (Gubbins 1999). The ocean floors and lake sediments are one of the only, albeit imperfect, record of these geomagnetic events (Merrill et al. 1996; Valet 2003). The occurrence of reversals is not constant through time, with intervals between such phenomena ranging from less than 0.1 million years to some 50 million years. Reversal frequency has increased during the last 85 million years, after the long interval of normal polarity during the Cretaceous. The last geomagnetic reversal, known as the Brunhes-Matuyama reversal occurred about 780000 years ago. It is remarkable to note that recent estimates indicate the actual directional shift between the two opposite polarities lasted less than 1000 years (Valet et al. 2012). Recently, investigating this event, Sagnotti et al. (2014) advance the debated idea that this polarity reversal occurred even in a shorter time, a fraction of a century.

4.1 Secular Variation and Secular Acceleration

The secular variation, defined as the first temporal derivative of the core field, carries information about the dynamics of the core. Directly, the secular variation can be computed from measurements at magnetic observatories, some of which have been around for more than one hundred years. Over longer times only long series of magnetic declination exist, such as those which have been compiled and given here in chronological order, by Malin and Bullard (1981), Cafarella et al. (1992), Barraclough (1995), Alexandrescu et al. (1996) and Korte et al. (2009) for London, Rome, Edinburgh, Paris and Munich, respectively (see Fig. 1).

In the following we however focus on the most recent variations, with some references to historical field variations. We also make a continuous link between the magnetic field behavior at the Earth's surface and at the core-mantle boundary, without a particular focus on the topic of core flow modeling. This choice is twofold: (i) firstly, over the last decades the magnetic field variations have been better and better described, at the global scale, due to availability of satellite data; (ii) secondly, for the purpose of this review, the rapid variations of the core field are the most interesting and appropriate to be described, considering the space weather/climatology time-scales.

A geomagnetic field model defining the core field and its secular variation can be downward continued to the core-mantle boundary, considering the mantle as an insulator from an electromagnetic point of view. We can then express the Gauss coefficients describing the core field and its secular variation at the Earth's surface into descriptions of the field at the core-mantle boundary and produce maps describing their spatial variations. The radial (or vertical) component is usually considered, the one which is continuous through this limit and which is used in computing flows at the top of the core. Figure 4 shows a map of the radial component of the main field and its secular variation at the top of the core for epoch 2005.0, as obtained from the model by Lesur et al. (2015). One of the most recent models, CHAOS-6 (Finlay et al. 2016a, 2016b) captures the secular variation up to at least spherical harmonic degree 16 (though the smaller length-scales mainly consist in time-averaged values).

At the core-mantle boundary, the secular variation map displays a different behavior over the Atlantic and Pacific hemispheres. In the Atlantic hemisphere the variations are very

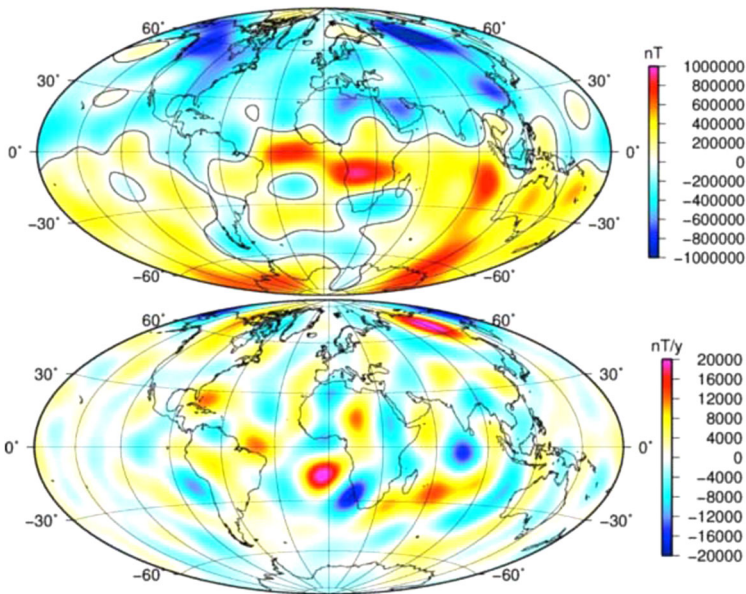


Fig. 4 Radial component of the core magnetic field and its secular variation at the core-mantle boundary as obtained from the model by Lesur et al. (2015)

important, up to some 10000 nT/yr, mainly in a region centered on the southern African continent, indicating very active core dynamics. The Pacific hemisphere remains, generally at the same low rate of secular variation, as well as the southern polar region. A combined explanation of the westward drift and hemispherical localisation of the secular variation is provided by Aubert et al. (2013).

It is interesting to compare the completely different behavior of the secular variation over the polar regions, with strong pairs of secular variation patches in the northern polar region. Some analysis of the regional secular variation inferred core upwelling in the northern polar region where reversed flux patches have been detected (see Fig. 5). Olson and Aurnou (1999) find a persistent westward polar vortex and a fluid upwelling inside the tangent cylinder, and Chulliat et al. (2010a, 2010b) note the existence of a bipolar secular variation structure situated at an emerging reversed flux patch and consider it as a harbinger of an upwelling and magnetic flux expulsion by radial diffusion. Amit (2014) shows that the geomagnetic secular variation morphology, in particular at some specific core-mantle boundary regions, may reflect the kinematics of magnetic field stretching by fluid upwelling or downwelling.

The origin of the reversed flux patches has been an outstanding question; previously they had been attributed to westward motion of a large flux patch under Siberia (Bloxham and Gubbins 1985). Recently, Livermore et al. (2017) considering the dynamical regime of the core, suggest that this behavior can be linked to a localized westward cylindrical jet of about 400 km width centered on the tangent cylinder. Since the epoch 2000, they argue that its strength has increased by a factor of three. Let us note here that the whole core flow geometry, including the local jet has been revealed by Pais and Jault (2008). Computing core flows from high resolution secular variation models, these authors show the presence of a large jet encircling the inner core, which carries an important part of the core angular momentum.

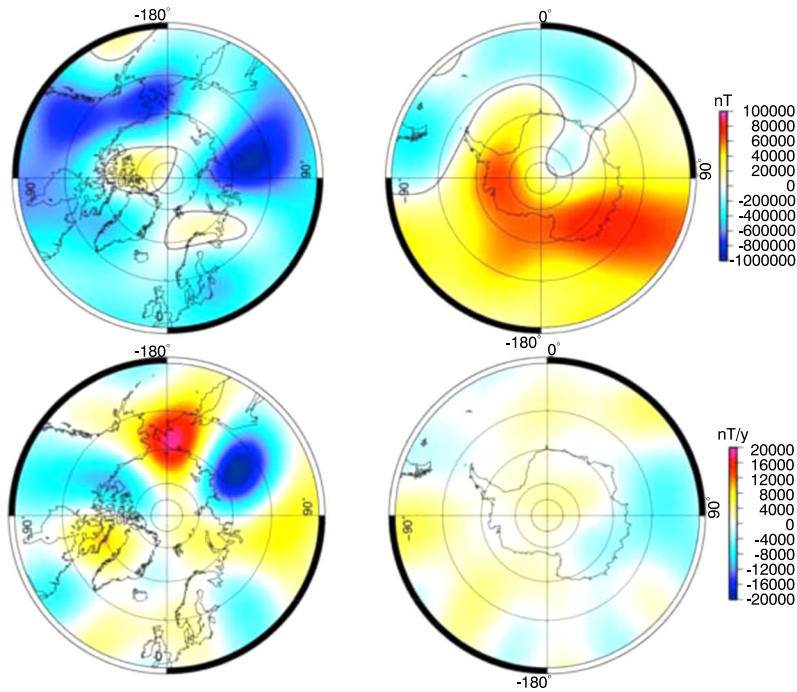


Fig. 5 Radial component of the magnetic field and its secular variation at the core-mantle boundary as obtained from the model by Lesur et al. (2015). Polar projection

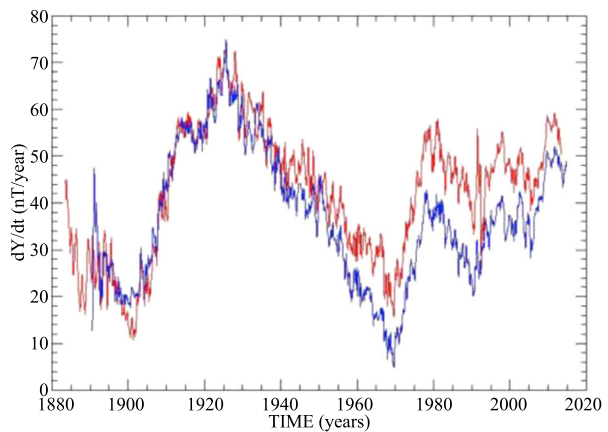
For the secular variation the characteristic time-scale is considered of the order of a century and may reflect the convective overturn time of the core (Christensen et al. 2012). The shortest observable time-scales over a decade or less could be related to fast torsional waves (Gillet et al. 2010; Asari and Lesur 2011). Christensen et al. (2012) suggest from the analysis of geodynamo simulations that core dynamics at short time-scales (decadal and subdecadal) is conducted by processes similar to those at centennial timescales. The short timescale features presently observed in the satellite-based models have been connected to the possible mechanism through which geomagnetic jerks occur (Olsen and Manda 2007; Wardinski et al. 2008; Chulliat et al. 2010a, 2010b; Finlay et al. 2016a, 2016b).

4.2 Rapid Fluctuations and Geomagnetic Jerks

Geomagnetic jerks are sharp changes in the trend of the first-time derivative of the magnetic field corresponding to abrupt jumps in the second-time derivative (e.g. Manda et al. 2010). The secular variation and geomagnetic jerks then appear as a series of nearly straight lines separated by these events, as seen in Fig. 6 for the East (Y) component at two European observatories, Chambon la Forêt and Niemegek, located respectively in France and Germany. It is interesting to note the different behavior after 1940, when the rate of secular variation is different between the two locations.

During the past nearly two decades when high quality satellite data has been available the core secular variation and secular acceleration have been described to high spherical harmonic degree, reliable up to degree-order 16. This allows a focus on explaining rapid core field variations on a global scale. At Earth's surface, large-scale patterns of secular

Fig. 6 Secular variation as obtained from monthly means at Chambon la Forêt (*red curve*) and Niemegk (*blue curve*) observatories



acceleration change on short, sub-decadal timescales. To better describe these rapid changes, time series of monthly point estimates at satellite altitude have been proposed and exploited, as “virtual observatories” (Mandea and Olsen 2006; Whaler and Beggan 2015; Saturnino et al. 2017). This new concept allows us to observe geomagnetic jerks directly in satellite data. Satellite data also reveal secular acceleration pulses in the Earth’s geomagnetic field (Chulliat et al. 2010a, 2010b). The most recent events in 2007 and 2012 appear to have their origin in a succession of core field acceleration pulses occurring predominantly in West Africa and the South Atlantic region (Chulliat and Maus 2014; Finlay et al. 2015). The last reported jerk is in 2014 (Torta et al. 2015) occurred as a strong secular acceleration in the Africa–South Atlantic region, extending into Europe.

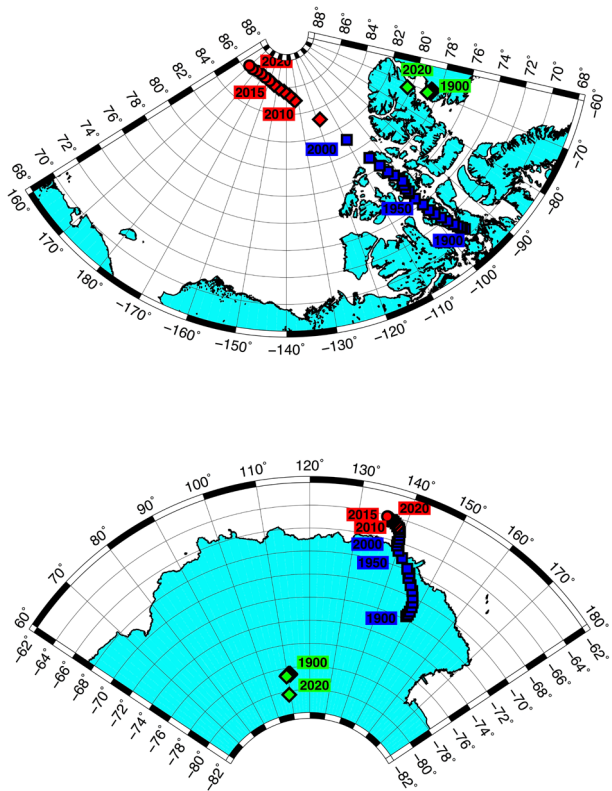
In spite of many attempts, the physical origin of these events is not yet fully established. Torsional waves have often been considered as the main source of the intense and rapidly changing patterns evident in the secular variation. Recently, however, Gillet et al. (2015a, 2015b) suggest that enhanced non-zonal flow at low latitudes, particularly around 90°W , as well as 60 and 120°E appear to be responsible. Whether the secular variation is due to wave or advection is a controversial issue, and likely it is a combination of both. How to separate the signal due to waves from the signal due to advection by the flow can take advantage of the new magnetic observations provided by satellite missions as well as the new advanced numerical simulations.

Finally, let us recall that geomagnetic jerk occurrences may be linked to other geophysical phenomena, such as sudden changes in the length of the day (Olsen and Mandea 2008; Mandea et al. 2010; Holme and de Viron 2013), or to changes in the phase of the free core nutation (Malkin 2013). We can notice here the complexity of these phenomena, and the importance of understanding their possible multiple origins, especially when considering topics such as space weather.

4.3 Specific Core Features and Their Temporal Variations

Some specific features linked to the core field and its variations are of signal importance to space weather, such as the location of the magnetic poles, the dipole moment decay, and the SAA. The locations of the magnetic poles controls the locations of the northern and southern cusps of the magnetosphere. The dipole moment decay, and the associated increase in size and deepening of the SAA, have important consequences with respect to radiation damage of satellites, and the electric power grid.

Fig. 7 Magnetic dip (blue and red) and dipole (green) positions as obtained from IGRF-12 model

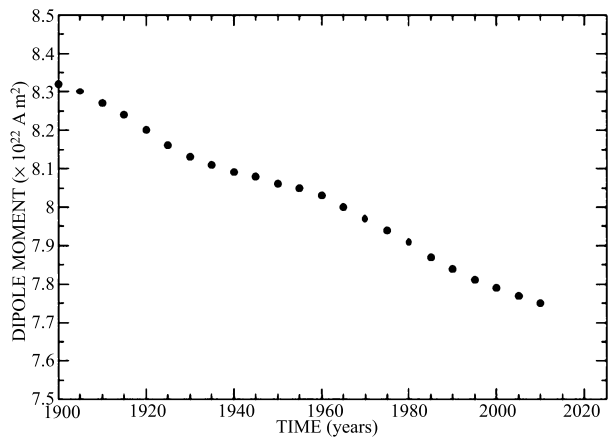


Magnetic Poles The positions of the north and south magnetic poles gradually change. Using the *gufm* model (Jackson et al. 2000) or recent IGRF models (Thébault et al. 2015), the locations and velocities for the two magnetic poles can be computed. Such computations indicate that over more than 400 years both magnetic poles have changed their positions. However, the rate for each pole is very different, and the movement depends on whether the pole is calculated solely from the dipole term, or from the entire spherical harmonic series (termed the dip pole). The symmetry of the auroral oval, at the boundary of open and closed magnetic field lines, is dominated by the dipole term because the proximal source of the aurora components is in the Earth's magnetic tail. Higher order magnetic components decay faster than the dipole term, and in the magnetic tail, the dipole term is dominant. For longer time-scales, the geomagnetic and magnetic pole locations from 7000 BC to A.D. 2006.6 are discussed in Korte and Manda (2008).

Over the last century, the magnetic dip poles have been moving in a northwest direction. During the first half of the 20th century their velocity was comparable, around some 5–10 km/yr. Since 1970, the time of a well-documented geomagnetic jerk, the north magnetic pole has moved from Canada towards Siberia, with velocities reaching some 60 km/yr (Newitt et al. 2002; Olsen and Manda 2007) and the south magnetic pole towards Australia, with a much lower velocity of around 5 km/yr.

Figure 7 shows the magnetic poles positions as obtained from IGRF models. A striking feature appears for the north magnetic pole velocity, which stopped its advance, entering into a deceleration phase, its velocity decreasing from about 53 km/yr in 2015 to an estimated

Fig. 8 Geomagnetic dipole moment as computed from the IGRF-12 model



value of 43 km/yr in 2020 (but note that the latter value relies on the predictive secular variation).

A glance over the last century of the rapid change in the north magnetic pole positions can be thought to be a signature of a sudden change in the behavior of the field, which has some signatures of an early phase of a field reversal. However, in the other hemisphere the south magnetic pole has kept nearly the same velocity rate (Mandea and Dormy 2003).

Dipole Moment Decay As discussed previously, direct intensity measurements are available since Gauss elaborated a method for determining intensity in 1832. These measurements allow us to compute the dipolar field, and its dominant axial part, parallel to the Earth's rotation axis. The dipole moment has decreased by nearly 6% per century since intensity magnetic field measurements exist. Figure 8 shows the axial component of the dipole field as computed from the IGRF field model. The general decreasing rate is of some 16 nT/yr. However, at some epochs the field has very different rate fluctuations. For example around 1980, it diminished twice as fast as nowadays. If the same rate of decay is extrapolated in time, the axial dipole would reach zero in less than 2000 yrs.

A question arises: what may be the future evolution and the implications of this significant dipole moment decay? To offer possible answers it is crucial to understand the physical process responsible for the dipole moment decay. Fluid motion in the outer core transport magnetic field lines, converting kinetic energy into magnetic energy. This ensures the maintenance of the magnetic field against Ohmic dissipation. Considering the free decay of the dipole, if the fluid motions ceased, it is estimated that in some 55000 years the axial dipole would reach a zero level. This time interval is more than one order of magnitude larger than the value of 2000 yrs., based on recent observations. An explanation could be found in proposed scenarios by Finlay et al. (2016a, 2016b) for the fluid motions within the core.

South Atlantic Anomaly One of the striking characteristics of the geomagnetic field is named the South Atlantic Anomaly, the region where the total field intensity is unusually low and the particle flux unusually high (Fig. 9), with a minimum value of about 22,000 nT for the epoch 2015. That minimum is situated close to the Paraguayan city of Asuncion. This central minimum has moved from southern Africa to South America (Mandea et al. 2007) in the recent past. Comparing MAGSAT and CHAMP satellite measurements, as well as considering only Swarm measurements, it has been possible to estimate the core field

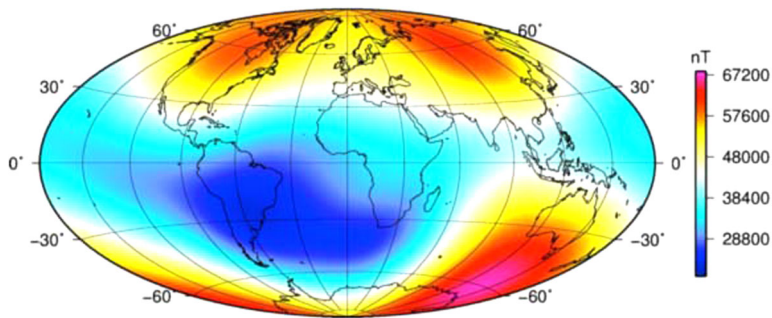


Fig. 9 Map of the total field intensity at the Earth's surface. The South Atlantic Anomaly is defined as the region of the lowest magnetic field values

intensity changes. The result indicates that the field strength has dramatically changed over the last decades, in a region situated again on the southern Atlantic Ocean–African sub-continent, by nearly 1%/yr.

The SAA is not only a characteristic of the present geo-magnetic field but it has been observed during the last four centuries (Jackson et al. 2000). Over longer time-scales the model resolution does not allow a well-determined description of its spatial variations. However, it is also present in the CALSxK series of models (based on paleo- and archeomagnetic data) with different locations and morphologies (Korte et al. 2011).

The SAA behavior seems to indicate that it might be connected to the general decrease of the dipole moment and to the significant increase of the non-dipolar field in this region. The weakness of the field intensity is caused by an increasing patch of opposite magnetic flux compared to the dipole direction at the core-mantle boundary. Pavón-Carrasco and De Santis (2016) analyze in detail the behavior of the SAA over the last 200 yrs. Their results indicate that one of the reversed polarity patches located under the South Atlantic Ocean grew with a rate of 2.54×10^5 nT per century. At the same time the quadrupole field seems to control this decreasing field strength. This behavior is similar to that obtained by numerical modeling, i.e. a reversal is preceded by the development of reverse flux patches at low-mid latitude, which migrates poleward and reduce the axial dipolar field (Wicht et al. 2010). However, the current value of the dipole moment is not as low as the mean moment in the Holocene.

The importance of understanding the evolution of the South Atlantic Anomaly for space weather is evident. This regional weakening in field intensity allows energetic particles and cosmic rays to penetrate much deeper into the magnetosphere than in other regions, resulting in significant space weather effects, such as satellite outages, even affecting ground-based systems. As a space weather phenomena, Geomagnetically Induced Currents (GIC) impact ground-based technological structures at all latitudes. Recently, Barbosa et al. (2015), investigating GIC occurrences in the power networks at low latitudes in the central Brazilian region, show significant effects in these regions during solar cycles 23 and 24.

5 Conclusions and Future Directions

A comprehensive separation and understanding of the internal and external processes contributing to the Earth's magnetic fields is crucial for space weather research. Continuous monitoring of the magnetic field, combining ground and space platforms, aims to address such needs.

What can the practice of space weather learn from current research in geomagnetism? Two first order features of the geomagnetic field, the rapid decay of the dipole field, and the expansion of the South Atlantic Anomaly, are of prime importance to space weather because they accentuate the impact of space weather events. Both of these features point to the importance of combining data assimilation approaches (Fournier et al. 2010) to geomagnetic weather prediction with experimental approaches to determine more of the state vector at the core mantle boundary, and a better understanding of its mean state. That means investing in experimental dynamos that are good analogs to the Earth's outer core, and in forecasting and hindcasting of the geomagnetic field. Understanding the puzzling processes that produce geomagnetic jerks also hold the promise of a deeper understanding of the mean state of the core.

Acknowledgements We thank N. Gillet for valuable comments and V. Lesur for providing GRIMM model inputs. Data collected at magnetic observatories Chambon la Foret and Niemegk were used, and we thank the observatory staff for providing them (BCMT: doi:10.18715/BCMT.MAG.DEF). Part of this was supported by a grant of the Ministry of National Education and Scientific Research, RDI Programme for Space Technology and Advanced Research—STAR, project number 513. We gratefully acknowledge constructive suggestions from two anonymous reviewers.

Appendix

Table 1 Attributes of recent geomagnetic field models

	Version	Comp. ^a	S.H. degree ^b	Data ^c	Selec. ^d	Ref.	Web ^e	Usable ^f	Uses ^g
CM	5	In, Io, T, M, O	107/20/60/1	S, Sg, O	Q, D	Sabaka et al. (2015)	1	≤1000 km	R., Sw V
CHAOS	4	In, M	85/16/−/2	S, Om	Q	Olsen et al. (2014)	2	≤1000 km	R.
GRIMM	2	In, M	30/16/−/2	S, O	Q	Lesur et al. (2010)	3	CMB	R., CMB
IGRF	12	In	13/8/−/−	S, Om	Q	Thébault et al. (2015)	4	≤1000 km	Navigation

^aComponents explanation: In = Internal (core and lithosphere) components; Io = Ionosphere and associated induced components; T = Toroidal components; M = Magnetosphere and associated induced components; O = Oceanic M2 tide

^bS. H. (Spherical Harmonic) degree expansion: 1st number is the degree of the spatial expansion for core and lithospheric fields; 2nd number is the maximum degree for the time varying core field; 3rd number is the maximum degree of the ionospheric field expansion; 4th number is the maximum degree of the magnetospheric field expansion

^cData explanation: S = Satellite vector and scalar data (CHAMP, Ørsted, SAC-C or some subset); Sg = Along-track satellite gradient data; O = Observatory hourly mean values; Om = Observatory monthly mean values

^dSelection explanation: Selection indicates whether quiet (Q) and/or Disturbed (D) data have been used in the model

^eWebpages: 1 = www.planetary-mag.net/planets.html (for the previous CM model, CM4); 2 = www.spacecenter.dk/files/magnetic-models/CHAOS-6; 3 = www.gfz-potsdam.de/magmodels; 4 = www.ngdc.noaa.gov/IAGA/vmod/igrf.html

^fUsable: Region where the model is pertinent; CMB = Core mantle boundary

^gUses: Specific use of the models; R = Research; Sw V = Swarm validation; CMB = Core mantle boundary

References

- M.M. Adams, D.R. Stone, D.S. Zimmerman, D.P. Lathrop, Liquid sodium models of the Earth's core. *Prog. Earth Planet. Sci.* (2015). doi:[10.1186/s40645-015-0058-1](https://doi.org/10.1186/s40645-015-0058-1)
- M. Alexandrescu, V. Courtillot, J.L. Le Mouél, Geomagnetic field direction in Paris since the mid-sixteenth century. *Phys. Earth Planet. Inter.* **98**, 321–360 (1996)
- H. Amit, Can downwelling at the top of the Earth's core be detected in the geomagnetic secular variation? *Phys. Earth Planet. Inter.* **229**, 110–121 (2014). doi:[10.1016/j.pepi.2014.01.012](https://doi.org/10.1016/j.pepi.2014.01.012)
- S. Asari, V. Lesur, Radial vorticity constraint in core flow modeling. *J. Geophys. Res.* **116**, B11101 (2011). doi:[10.1029/2011JB008267](https://doi.org/10.1029/2011JB008267)
- J. Aubert, Geomagnetic forecasts driven by thermal wind dynamics in the Earth's core. *Geophys. J. Int.* **203**(3), 1738–1751 (2015). doi:[10.1093/gji/ggv394](https://doi.org/10.1093/gji/ggv394)
- J. Aubert, C.C. Finlay, A. Fournier, Bottom-up control of geomagnetic secular variation by the Earth's inner core. *Nature* **502**, 219–223 (2013). doi:[10.1038/nature12574](https://doi.org/10.1038/nature12574)
- C. Barbosa, L. Alves, R. Carballo, G.A. Hartmann, A.R.R. Papa, R.J. Pirjola, Analysis of geomagnetically induced currents at a low-latitude region over the solar cycles 23 and 24: comparison between measurements and calculations. *J. Space Weather Space Clim.* **5**, A35 (2015). doi:[10.1051/swsc/2015036](https://doi.org/10.1051/swsc/2015036)
- D. Barraclough, Observations of the Earth's magnetic field in Edinburgh, from 1670 to the present day. *Trans. R. Soc. Edinb. Earth Sci.* **85**, 239–252 (1995)
- J. Bloxham, D. Gubbins, The secular variation of Earth's magnetic field. *Nature* **317**, 777–781 (1985)
- L. Cafarella, A. De Santis, A. Meloni, Secular variation in Italy from historical geomagnetic field measurements. *Phys. Earth Planet. Inter.* **73**, 206–221 (1992)
- W.H. Campbell, *Introduction to Geomagnetic Fields* (Cambridge Univ. Press, New York, 2003), 304 pp. CHAMP, <http://www.gfz-potsdam.de/champ/>. Accessed Sept. 2017
- U.R. Christensen, I. Wardinski, V. Lesur, Timescales of geomagnetic secular acceleration in satellite field models and geodynamo models. *Geophys. J. Int.* **190**(1), 243–254 (2012). doi:[10.1111/j.1365-246X.2012.05508.x](https://doi.org/10.1111/j.1365-246X.2012.05508.x)
- A. Chulliat, S. Maus, Geomagnetic secular acceleration, jerks, and a localized standing wave at the core surface from 2000 to 2010. *J. Geophys. Res.* (2014). doi:[10.1002/2013JB010604](https://doi.org/10.1002/2013JB010604)
- A. Chulliat, G. Hulot, L. Newitt, Magnetic flux expulsion from the core as a possible cause of the unusually large acceleration of the north magnetic pole during the 1990s. *J. Geophys. Res.* **115** (2010a). doi:[10.1029/2009JB007143](https://doi.org/10.1029/2009JB007143)
- A. Chulliat, E. Thébaud, G. Hulot, Core field acceleration pulse as a common cause of the 2003 and 2007 geomagnetic jerks. *Geophys. Res. Lett.* (2010b). doi:[10.1029/2009GL042019](https://doi.org/10.1029/2009GL042019)
- E.W. Cliver, W. Dietrich, The 1859 space weather event revisited: limits of extreme activity. *J. Space Weather Space Clim.* **3**, 15 (2013)
- Cluster, <http://sci.esa.int/cluster/>. Accessed Nov. 2017
- ESA, http://www.esa.int/Our_Activities/Observing_the_Earth/Swarm. Accessed Sept. 2017
- C.C. Finlay, A. Jackson, N. Gillet, N. Olsen, Core surface magnetic field evolution 2000–2010. *Geophys. J. Int.* **189**, 761–781 (2012). doi:[10.1111/j.1365-246X.2012.05395.x](https://doi.org/10.1111/j.1365-246X.2012.05395.x)
- C.C. Finlay, N. Olsen, L. Tøffner-Clausen, DTU candidate field models for IGRF-12 and the CHAOS-5 geomagnetic field model. *Earth Planets Space* **67**, 114 (2015). doi:[10.1186/s40623-015-0274-3](https://doi.org/10.1186/s40623-015-0274-3)
- C.C. Finlay, J. Aubert, N. Gillet, Gyre-driven decay of the Earth's magnetic dipole. *Nat. Commun.* (2016a). doi:[10.1038/ncomms10422](https://doi.org/10.1038/ncomms10422)
- C.C. Finlay, N. Olsen, S. Kotsiaros, N. Gillet et al., Recent geomagnetic secular variation from swarm and ground observatories as estimated in the CHAOS-6 geomagnetic field model. *Earth Planets Space* **68**, 112 (2016b). doi:[10.1186/s40623-016-0486-1](https://doi.org/10.1186/s40623-016-0486-1)
- A. Fournier, G. Hulot, D. Gault, W. Kuang, A. Tangborn, N. Gillet, E. Canet, J. Aubert, F. Lhuillier, An introduction to data assimilation and predictability in geomagnetism. *Space Sci. Rev.* **155**, 247–291 (2010)
- N. Gillet, D. Jault, E. Canet, A. Fournier, Fast torsional waves and strong magnetic field within the Earth's core. *Nature* **465**, 74–77 (2010). doi:[10.1038/nature09010](https://doi.org/10.1038/nature09010)
- N. Gillet, D. Jault, C.C. Finlay, Planetary gyre, time dependent eddies, torsional waves, and equatorial jets at the Earth's core surface. *J. Geophys. Res., Solid Earth* **120**(6), 3991–4013 (2015a)
- N. Gillet, O. Barrois, C.C. Finlay, Stochastic forecasting of the geomagnetic field from the COV-OBS.x1 geomagnetic field model, and candidate models for IGRF-12. *Earth Planets Space* **67**, 71 (2015b). doi:[10.1186/s40623-015-0225-z](https://doi.org/10.1186/s40623-015-0225-z)
- D. Gubbins, The distinction between geomagnetic excursions and reversals. *Geophys. J. Int.* **137**, 1–3 (1999)
- R. Holme, O. de Viron, Characterization and implications of intradecadal variations in length of day. *Nature* **499**, 202–204 (2013). doi:[10.1038/nature12282](https://doi.org/10.1038/nature12282)

- G. Hulot, *The Swarm Delta NanoMagSat Project, Latest News, IAPSO-IAMAS-IAGA 2017 Scientific Assembly* (2017)
- G. Hulot, T. Sabaka, N. Olsen, A. Fournier, The present and future geomagnetic field, in *Treatise on Geophysics, Geomagnetism*, 2nd edn., ed. by M. Kono (Elsevier, Amsterdam, 2015), pp. 33–78
- Intermagnet, www.intermagnet.org. Accessed Sept 2017
- A. Jackson, A.R.T. Jonkers, M.R. Walker, Four centuries of geomagnetic secular variation from historical records. *Philos. Trans. R. Soc. Lond. A* **358**, 957–990 (2000)
- T. Kane, P. Hillman, C. Denman, M. Hart, R. Scott, M. Purucker, S. Potashnik, Laser remote magnetometry using mesospheric sodium (2016). [arXiv:1610.05385v2](https://arxiv.org/abs/1610.05385v2)
- M. Korte, M. Manda, Magnetic poles and dipole tilt variation over the past decades to millennia. *Earth Planets Space* **60**, 937–948 (2008)
- M. Korte, M. Manda, J. Matzka, A historical declination curve for Munich from different data sources. *Phys. Earth Planet. Inter.* **174**, 161–172 (2009)
- M. Korte, C. Constable, F. Donadini, R. Holme, Reconstructing the Holocene geomagnetic field. *Earth Planet. Sci. Lett.* **312**, 497–505 (2011). doi:[10.1016/j.epsl.2011.10.031](https://doi.org/10.1016/j.epsl.2011.10.031)
- J.M. Leger, F. Bertrand, T. Jager, M. Le Prado, I. Fratter, J.C. Lalaurie, Swarm absolute scalar and vector magnetometer based on helium 4 optical pumping, in *Proceedings of the EuroSensors XXIII Conference 1:1* (2009), pp. 634–637. doi:[10.1016/j.proche.2009.07.158](https://doi.org/10.1016/j.proche.2009.07.158)
- V. Lesur, I. Wardinski, S. Asari, B. Minchev, M. Manda, Modelling the earth's core magnetic field under flow constraints. *Earth Planets Space* **62** (2010)
- V. Lesur, K. Whaler, I. Wardinski, Are geomagnetic data consistent with stably stratified flow at the core-mantle boundary? *Geophys. J. Int.* 929–946 (2015). doi:[10.1093/gji/ggv031](https://doi.org/10.1093/gji/ggv031)
- P.W. Livermore, R. Hollerbach, C.C. Finlay, An accelerating high-latitude jet in Earth's core. *Nat. Geosci.* **10**, 62–68 (2017). doi:[10.1038/ngeo2859](https://doi.org/10.1038/ngeo2859)
- F.J. Lowes, Mean-square values on sphere of spherical harmonic vector fields. *J. Geophys. Res.* **71**, 2179 (1966)
- S.R.C. Malin, E. Bullard, The direction of the Earth's magnetic field at London, 1570–1975. *Philos. Trans. R. Soc. Lond.* **299**, 357–423 (1981)
- Z. Malkin, Free core nutation and geomagnetic jerks. *J. Geodyn.* **72**, 53–58 (2013). doi:[10.1016/j.jog.2013.06.001](https://doi.org/10.1016/j.jog.2013.06.001)
- M. Manda, E. Dormy, Asymmetric behaviour of magnetic dip poles. *Earth Planets Space* **55**, 153–157 (2003)
- M. Manda, J.L. Le Mouél, After some 350 years—zero declination again in Paris. *Hist. Geo- Space Sci.* (2016)
- M. Manda, N. Olsen, A new approach to directly determine the secular variation from magnetic satellite observations. *Geophys. Res. Lett.* **33**, L15306 (2006). doi:[10.1029/2006GL026616](https://doi.org/10.1029/2006GL026616)
- M. Manda, M. Korte, D. Mozzoni, P. Kotzé, The magnetic field changing over the Southern African continent—a unique behaviour. *S. Afr. J. Geol.* **110**, 193–202 (2007)
- M. Manda, R. Holme, A. Pais, K. Pinheiro, A. Jackson, G. Verbanac, Geomagnetic jerks: rapid core field variations and core dynamics. *Space Sci. Rev.* **155**, 147–175 (2010). doi:[10.1007/s11214-010-9663-x](https://doi.org/10.1007/s11214-010-9663-x)
- R.T. Merrill, M.W. McElhinny, P.L. McFadden, *The Magnetic Field of the Earth* (Academic Press, London, 1996)
- MMS, <http://mms.gsfc.nasa.gov>. Accessed Nov. 2017
- Natural Resources Canada, Space Weather, <http://spaceweather.gc.ca/sbg-en.php>. Accessed 7 Sep. 2017
- L. Newitt, M. Manda, L. McKee, J.J. Orgeval, Recent acceleration of the North magnetic pole linked to magnetic jerks. *Eos Trans. AGU* **83**(35), 381–389 (2002)
- N. Olsen, M. Manda, Will the magnetic north pole wind up in Siberia? *EOS* (2007)
- N. Olsen, M. Manda, Rapidly changing flows in the Earth's core. *Nat. Geosci.* **1**, 390–394 (2008). doi:[10.1038/ngeo203](https://doi.org/10.1038/ngeo203)
- N. Olsen, H. Lühr, C. Finlay, T. Sabaka, I. Michaelis, L. Tøffner-Clausen, The CHAOS-4 geomagnetic field model. *Geophys. J. Int.* **197**, 815–827 (2014). doi:[10.1093/gji/ggu033](https://doi.org/10.1093/gji/ggu033)
- P. Olson, J. Aurnou, A polar vortex in the Earth's core. *Nature* **402**, 170–173 (1999)
- Ørsted, [https://en.wikipedia.org/wiki/Ørsted_\(satellite\)](https://en.wikipedia.org/wiki/Ørsted_(satellite)). Accessed Sept. 2017
- M.A. Pais, D. Jault, Quasi-geostrophic flows responsible for the secular variation of the Earth's magnetic field. *Geophys. J. Int.* **173**, 421–443 (2008)
- F.J. Pavón-Carrasco, A. De Santis, The South Atlantic Anomaly: the key for a possible geomagnetic reversal. *Front. Earth Sci.* **4** (2016). doi:[10.3389/feart.2016.00040](https://doi.org/10.3389/feart.2016.00040)
- M. Purucker, K. Whaler, Crustal magnetism, in *Treatise on Geophysics, Geomagnetism*, 2nd edn., ed. by M. Kono (Elsevier, Amsterdam, 2015), pp. 185–218
- RBSP, http://www.nasa.gov/mission_pages/rbsp/mission/. Accessed Nov. 2017

- T. Sabaka, N. Olsen, R. Tyler, A. Kuvshinov, CM5, a pre-Swarm comprehensive geomagnetic field model derived from over 12 yr of CHAMP, Ørsted and SAC-C data. *Geophys. J. Int.* **200**, 1596–1626 (2015). doi:[10.1093/gji/ggu493](https://doi.org/10.1093/gji/ggu493)
- L. Sagnotti, G. Scardia, B. Giaccio, J.C. Liddicoat, S. Nomade, P.R. Renne, C.J. Sprain, Extremely rapid directional change during Matuyama–Brunhes geomagnetic polarity reversal. *Geophys. J. Int.* **199**(2), 1110–1124 (2014). doi:[10.1093/gji/ggu287](https://doi.org/10.1093/gji/ggu287)
- D. Saturnino, B. Langlais, H. Amit, F. Civet, M. Manda, E. Beucler, Combining virtual observatory and equivalent source dipole approaches to describe the geomagnetic field with Swarm measurements. *Phys. Earth Planet. Inter.* (2017). doi:[10.1016/j.pepi.2017.06.004](https://doi.org/10.1016/j.pepi.2017.06.004)
- E. Thébault, C.C. Finlay, C.D. Beggan, P. Alken, J. Aubert, O. Barrois, F. Bertrand, T. Bondar, A. Boness, L. Brocco, E. Canet, A. Chambodut, A. Chulliat, P. Coisson, F. Civet, A. Du, A. Fournier, I. Fratter, N. Gillet, B. Hamilton, M. Hamoudi, G. Hulot, T. Jager, M. Korte, W. Kuang, X. Lalanne, B. Langlais, J.M. Leger, V. Lesur, F.J. Lowes, S. Macmillan, M. Manda, C. Manoj, S. Maus, N. Olsen, V. Petrov, V. Ridley, M. Rother, T.J. Sabaka, D. Saturnino, R. Schachtschneider, O. Sirol, A. Tangborn, A. Thomson, L. Tøffner-Clausen, P. Vigneron, I. Wardinski, T. Zvereva, International geomagnetic reference field: the 12th generation. *Earth Planets Space* **67**(1), 1–19 (2015). doi:[10.1186/s40623-015-0228-9](https://doi.org/10.1186/s40623-015-0228-9)
- J.M. Torta, F.J. Pavón-Carrasco, S. Marsal, C.C. Finlay, Evidence for a new geomagnetic jerk in 2014. *Geophys. Res. Lett.* (2015). doi:[10.1002/2015GL065501](https://doi.org/10.1002/2015GL065501)
- J.P. Valet, Time variations in geomagnetic intensity. *Rev. Geophys.* (2003). doi:[10.1029/2001/RG000104](https://doi.org/10.1029/2001/RG000104)
- J.P. Valet, A. Fournier, V. Courtillot, E. Herrero-Bervera, Dynamical similarity of geomagnetic field reversals. *Nature* **490**(7418), 89–93 (2012)
- I. Wardinski, R. Holme, S. Asari, M. Manda, The 2003 geomagnetic jerk and its relation to the core surface flows. *Earth Planet. Sci. Lett.* **267**, 468–481 (2008). doi:[10.1016/j.epsl.2007.12.008](https://doi.org/10.1016/j.epsl.2007.12.008)
- K. Whaler, C. Beggan, Core Flow modelling using acceleration. *J. Geophys. Res., Solid Earth* **120**, 1400–1414 (2015). doi:[10.1002/2014JB011697](https://doi.org/10.1002/2014JB011697)
- J. Wicht, H. Harder, S. Stellmach, Numerical dynamo simulations—from basic concepts to realistic models, in *Handbook of Geomathematics*, ed. by W. Freeden, Z. Nashed, T. Sonar (Springer, Heidelberg, 2010)
- T. Wolf, P. Neumann, K. Nakamura, H. Sumiya, T. Ohshima, J. Isoya, J. Wrachtrup, Subpicotesla diamond magnetometry. *Phys. Rev. X* **5**, 041001 (2015). doi:[10.1103/PhysRevX.5.041001](https://doi.org/10.1103/PhysRevX.5.041001)